Colloids and Surfaces A: Physicochem. Eng. Aspects 339 (2009) 159–166

Contents lists available at ScienceDirect

Colloids and Surfaces A: Physicochemical and Engineering Aspects

journal homepage: www.elsevier.com/locate/colsurfa

Adsorption of Pb(II) on diatomite as affected via aqueous solution chemistry and temperature

Guodong Sheng[a,b], Suowei Wang[c], Jun Hu[a], Yi Lu[a], Jiaxing Li[a,*], Yunhui Dong[c], Xiangke Wang[a,b,*]

[a] Key Laboratory of Novel Thin Film Solar Cells, Institute of Plasma Physics, Chinese Academy of Sciences, P.O. Box 1126, 230031, Hefei, PR China
[b] School of Nuclear Science and Engineering, North China Electric Power University, 102206, Beijing, PR China
[c] School of Chemical Engineering, Shandong University of Technology, 255049, Zibo, PR China

ARTICLE INFO

Article history:
Received 22 October 2008
Received in revised form 8 February 2009
Accepted 12 February 2009
Available online 23 February 2009

Keywords:
Diatomite
Pb(II)
Adsorption
Thermodynamic data

ABSTRACT

To better understand the application of diatomite as an adsorbent for the removal of Pb(II) from heavy metal-contaminated water, in this paper, diatomite was used to adsorb Pb(II) from aqueous solution under various conditions. The results demonstrated that the adsorption of Pb(II) was strongly dependent on ionic strength at pH < 7.0, outer-sphere surface complexation or ion exchange may be the main adsorption mechanism of Pb(II) on diatomite at low pH values. No drastic difference of Pb(II) adsorption was observed at pH > 7.0, and the adsorption at high pH values was mainly dominated via inner-sphere surface complexation. The presence of HA/FA showed great influence on Pb(II) adsorption on diatomite. The adsorption of Pb(II) on diatomite was dependent on foreign ions (herein K^+, Na^+, ClO_4^-, NO_3^- and Cl^-) in solution at pH < 8.0, and was independent of foreign ions at pH > 8.0. The thermodynamic parameters (i.e., ΔH°, ΔS°, ΔG°) were evaluated from the temperature dependent adsorption isotherms. The results indicated that the adsorption process of Pb(II) on diatomite was spontaneous and endothermic in nature.

1. Introduction

Water contamination by hazardous metal ions is a worldwide problem [1,2]. Strict environmental protection legislation on the disposal of hazardous metal ions and increasing demands for water cleaning with fairly low level of hazardous metal ions make it greatly significant to exploit various effective techniques for hazardous metal ions removal. Recent studies mainly focused on the exploration of novel adsorbents with fast adsorption rate, large adsorption capacity, and high adsorption selectivity for hazardous metal ions. Numerous adsorbents such as activated carbon [3], synthetic resin [4], mesoporous silica [5], carbon nanotubes [6,7], natural and synthetic zeolite [8,9], clay minerals [10–12], natural and modified diatomite [13,14] and biomass [15] have been tested for their potential application to remove hazardous metal ions from wastewater. Among them, natural and modified diatomite is a promising adsorbent for the removal of hazardous metal ions in high efficiency and low cost because of its unique combination of physical and chemical properties. Dantas et al. [16] studied Cr^{3+} adsorption to crude and micro emulsion impregnated diatomite. Gürü et al. [17] studied the removal of Cr^{3+} from the artificial wastewater using low-cost diatomite in batch and continuous systems. Khraisheh et al. [14] examined the effectiveness of raw and modified diatomite for the uptake of Pb^{2+}, Cu^{2+} and Cd^{2+} from wastewater. Al-Degs et al. [18] studied the removal of Pb^{2+} by natural and manganese oxide modified diatomite. Khraisheh et al. [19] studied the removal of dyes from aqueous solution by raw and calcined diatomite. Yang et al. [20] evaluated the adsorption properties of urokinase on diatomite. The results demonstrated that diatomite was a very suitable adsorbent in wastewater management. However, to the best of our knowledge, only macroscopic adsorption data are available, little attention has been paid to the adsorption mechanism.

Despite of the extensive investigations on the adsorption of heavy metal ions [13,14,16–18] or organic compounds [19,20] on diatomite, according to our literature survey, there is still little information with respect to the influence of organic compounds on the adsorption of heavy metal ions. However, it should be noted that heavy metal ions and organic compounds exist simultaneously at many contaminated sites. For example, the presence of natural organic matter (NOM), such as humic acid (HA) and fulvic acid (FA), may influence the fate of heavy metal ions in natural environment. In our previous studies [21–24], the influence of HA/FA on heavy metal ions adsorption to minerals had been extensively studied. It

* Corresponding authors. Tel.: +86 551 5592788; fax: +86 551 5591310.
E-mail addresses: lijx@ipp.ac.cn (J. Li), xkwang@ipp.ac.cn (X. Wang).

0927-7757/$ – see front matter © 2009 Elsevier B.V. All rights reserved.
doi:10.1016/j.colsurfa.2009.02.016

was generally regarded that the adsorption was promoted at low pH values but declined at high pH values. However, the influence of HA/FA on heavy metal ions adsorption to diatomite is still scare. Therefore, to better understand the practical application of diatomite as a potential adsorbent in the wastewater management, it is greatly important to investigate the adsorption properties of heavy metal ions to diatomite in the presence of HA/FA.

In this work, we systematically investigated the adsorption properties of Pb(II) on diatomite under various solution chemistry conditions. Pb(II) was selected as a template heavy metal ion because of its extensive existence in water environment. The objectives of this work are: (1) to characterize the diatomite by X-ray powder diffraction (XRD), FTIR, N_2-BET and Zeta potential in detail; (2) to study the adsorption of Pb(II) on diatomite under various common conditions; (3) to calculate the thermodynamic data (ΔH°, ΔS°, ΔG°) from the temperature dependent adsorption isotherms and to evaluate the adsorption properties of Pb(II) on diatomite; (4) to draw together the relationship among pH, amount of Pb(II) adsorbed on diatomite and concentration of Pb(II) remained in solution; and (5) to discuss the adsorption mechanism of Pb(II) on diatomite.

2. Experimental

2.1. Chemicals

All chemicals were purchased in analytical purity and used without further purification. Doubly distilled water was used in all the experiments. The Pb(II) stock solution was prepared by dissolving $Pb(NO_3)_2$ in doubly distilled water and then diluted to 60 mg/L.

The sample of diatomite was achieved from Shengzhou county (Zhejiang province, China) and was characterized in detail. The sample was milled through a 200-mesh screen and then used in the experiments. Elemental analysis of diatomite was performed by plasma emission spectroscopy, and the predominant chemical components of diatomite are SiO_2 (65%), Al_2O_3 (17.5%), Fe_2O_3 (4.8%), Na_2O (0.5%) and CaO (1.1%), which are rather similar to those of Jordanian diatomite reported by Al-Degs et al. [18]. According to the potentiometric titration data, the sample of diatomite has two surface active sites, surface complexation site (XOH) and ion exchange site (XNa/K), the surface active site concentrations calculated with the aid of FITEQL 3.2 are 3.32×10^{-5} and 1.41×10^{-5} mol/g, respectively.

HA and FA were extracted from the soil of Hua-Jia county (Gansu province, China), and were characterized in detail [25–27]. Cross-polarization magic angle spinning (CPMAS) ^{13}C NMR spectra of HA and FA were divided into four chemical shift regions, i.e., 0–50, 51–105, 106–160 and 161–200 ppm. The four regions were referred to as aliphatic, carbohydrate, aromatic, and carboxyl regions. The percentage of the total intensity of each region was estimated by integrating CPMAS ^{13}C NMR spectra for each region. The fractions of aromatic groups calculated by expressing aromatic C as percentage of the sum of aliphatic C (0–105 ppm) and aromatic C (106–160 ppm) are tabulated in Table 1. In addition, the weight-averaged molecular weights (M_w) of dissolved HA and FA are evaluated according to the method of Chin et al. [28], and the M_w values of dissolved HA and FA are 2108 and 1364, respectively. The charge densities (Fig. 1) of dissolved HA and FA are calculated from the potentiometric titration data, and the results are quite similar to those reported by Bratskaya et al. [29].

Table 1
^{13}C NMR characteristics (chemical shift ppm) % of HA and FA[a].

	0–50	51–105	106–160	161–200	Aromaticity
HA	15	21	47	17	57
FA	16	28	19	39	30

[a] Refs. [26] and [27].

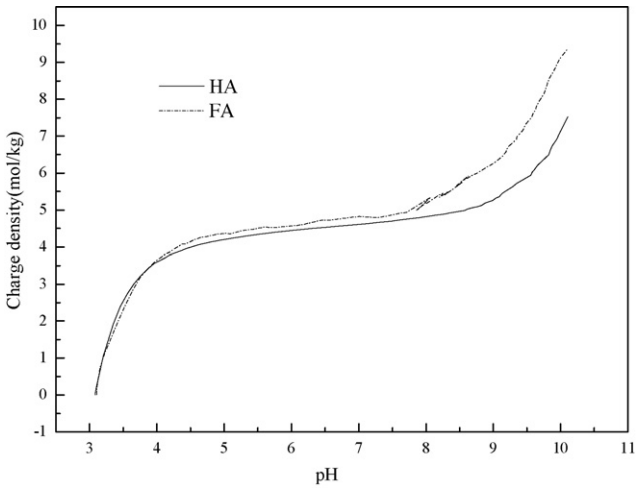

Fig. 1. Charge density profiles of dissolved HA and FA calculated from potentiometric titration data.

2.2. Characterization

The XRD analysis was performed with Cu K_α radiation ($\lambda = 0.154$ nm) on a Rigaku X-ray diffractometer. The IR measurements were mounted on a Bruker EQUINOX55 spectrometer in KBr pellet at room temperature. N_2-BET adsorption–desorption were determined at 77 K using Micromeritics ASAP 2010 equipment (BET and BJH models, respectively, for specific surface area and porosity evaluation) for diatomite samples. Before determination, the samples were degassed at 150 °C and 10^{-6} Torr. For Zeta potential analysis, the suspension of 2.5 g/L diatomite in 0.01 mol/L $NaClO_4$ solution was adjusted to an appropriate pH value by adding negligible amount of 0.01 mol/L $HClO_4$ or NaOH. The Zeta potential of the obtained suspension was then determined using a Zeta potential analyzer (Zetasizer Nano ZS, Malvern Co., UK). Each sample was measured with three independent determinations, and each determination was repeated for five times.

2.3. Adsorption procedures

The adsorption of Pb(II) on diatomite was investigated by using batch technique in polyethylene centrifuge tubes under ambient conditions. In all experiments, no attempt was made to exclude air. The diatomite suspension and $NaClO_4$ solution were pre-equilibrated for 24 h and then Pb(II) stock solution was added to achieve the desired concentration of the different components. The system was adjusted to the desired pH by adding negligible volumes of 0.01 or 0.1 mol/L $HClO_4$ or NaOH. After the suspensions were shaked for 48 h, the solid and liquid phases were separated by centrifugation at 9000 rpm for 40 min. The concentration of Pb(II) was determined by spectrophotometry at wavelength 616 nm by applying Pb(II)–Chlorophosphonazo(III) complex. To take into consideration the Pb(II) loss from procedures expect for diatomite adsorption (i.e., Pb(II) adsorption on centrifuge tube wall), calibration curves were attained separately under otherwise identical conditions as the adsorption process but no diatomite. Based on the attained calibration curves, the adsorbed mass of Pb(II) was calculated via subtracting the mass in the solution from the mass spiked. All experimental data were the average of duplicate or trip-

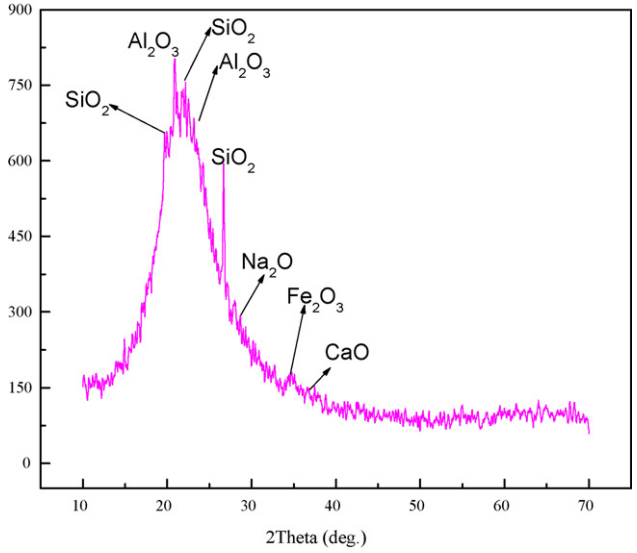

Fig. 2. XRD pattern of diatomite sample.

licate determinations. The relative errors of the data were about 5%.

3. Results and discussion

3.1. Characterization of diatomite

Fig. 2 shows the X-ray powder diffraction pattern of the raw diatomite. The diffraction spectrogram suggests that the raw diatomite consists mainly of silica (SiO_2) with a little of Al_2O_3, Fe_2O_3, CaO and Na_2O. The amorphous band described in Fig. 2 may be attributed to the glass formation of SiO_2, peaks at 19°, 21°, 26°, and 35° are the characteristic peaks of the diatomite [30]. The XRD diffraction gram shows that the raw diatomite is poorly crystallized. The structure of the sample is quite similar to that reported by Köseoglu et al. [30] (see also Fig. 2 in the reference).

Fig. 3 shows the infrared spectrum (IR) of the raw diatomite. The peaks at 3425 and 1630 cm^{-1} are corresponding to the stretching vibrations of adsorbed water and of zeolitic water,

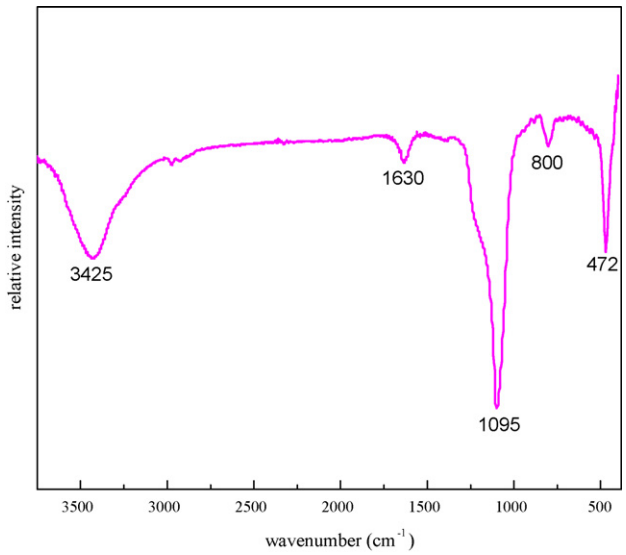

Fig. 3. FTIR spectrum of diatomite sample.

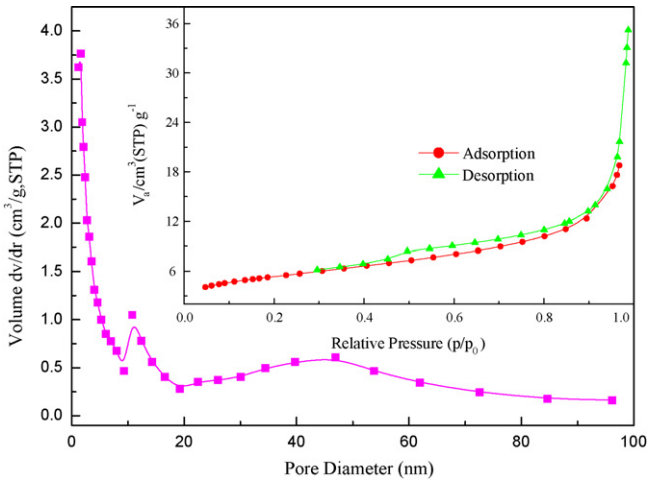

Fig. 4. N_2 adsorption–desorption isothermal (inset) and corresponding BJH pore-size distribution curve of diatomite sample, the pore-size distribution was calculated from the desorption branch of the isotherm.

respectively. The peaks at 472 and 1095 cm^{-1} may be attributed to the asymmetric stretching modes of Si–O–Si bonds, the peak at 800 cm^{-1} may correspond to the stretching vibration of Al–O–Si [31].

N_2 adsorption–desorption isotherms (inset figure in Fig. 4) and corresponding Barrett, Joyner and Halenda (BJH) pore-size distribution curve of diatomite sample are shown in Fig. 4. The stepwise adsorption and desorption isotherm is indicative of 3D intersection of a solid porous material [32]. The average pore size for the diatomite sample is 10.625 nm with a wide distribution of pore size. It is obvious that micropore is dominant of the total pore volume of the diatomite. The specific surface area and monolayer capacity of the diatomite are 18.8 m^2/g and 4.3 cm^3/g, respectively.

The Zeta potentials of diatomite sample at various pH values are illustrated in Fig. 5. It is clear that the Zeta potential of diatomite sample varies with the changing of pH. As is evidenced by the negative value of Zeta potential, the surfaces of diatomite are negatively charged in the wide pH range of 2–12, and the negative Zeta potential increases with increasing pH in this range, indicating that the quantity of negatively charged functional groups on the diatomite surface increases with pH rising, which is quite similar to the results reported by Gao et al. [33].

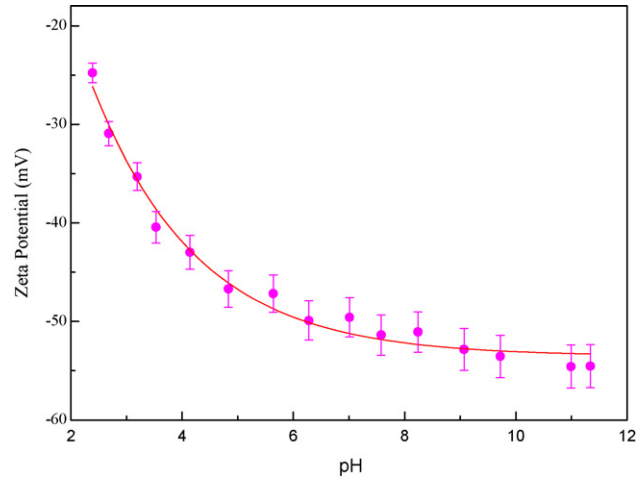

Fig. 5. Zeta potential of diatomite suspended in 0.01 mol/L $NaClO_4$ solution as a function of pH.

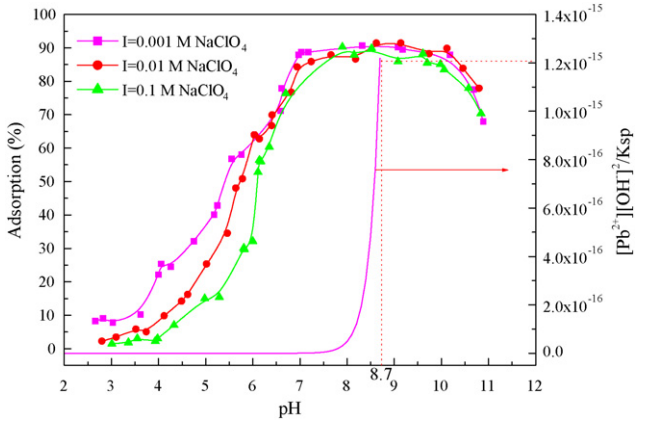

Fig. 6. Effect of ionic strength on Pb(II) adsorption on diatomite as a function of pH, adsorbent dosage = 0.2 g/L, initial Pb(II) concentration = 15 mg/L, T = 303.15 K.

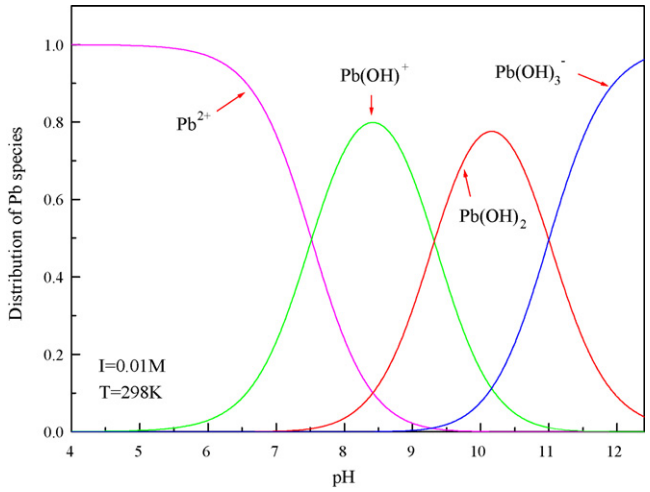

Fig. 7. Distribution of Pb(II) species as a function of pH based on the equilibrium constants.

3.2. Effect of pH and ionic strength

Adsorption percentage (%) was calculated from the difference between the initial concentration and the equilibrium one:

$$\text{Adsorption}\,\% = \frac{C_0 - C_e}{C_0} \times 100\% \quad (1)$$

where C_0 (mg/L) is the initial Pb(II) concentration, C_e (mg/L) is the concentration in supernatant after centrifugation.

It is well known that the removal of Pb(II) on diatomite from aqueous solutions by adsorption is significantly dependent on pH of solution, as it affects the surface charge of diatomite, the species of Pb(II) and the degree of ionization in solution. The effect of pH on the adsorption of Pb(II) on diatomite was conducted by varying pH from 2 to 12 at T = 303.15 K in 0.1, 0.01 and 0.001 mol/L $NaClO_4$ solutions, respectively. The results are shown in Fig. 6. In the pH range of 2.5–4.0, the adsorption percentage increases slightly as the pH increasing. The adsorption increases abruptly at pH 4.0–7.0, maintains a high level at pH 7.0–10.0, and then decreases sharply at pH > 10. The variation of solution pH before and after adsorption is also measured. The pH of the solution after adsorption changes a little to the acidic region, indicating that H^+ is released during the adsorption of Pb(II) on diatomite.

Weng [34] determined the relative distribution of Pb(II) species at ionic strength of 0.01 mol/L $NaClO_4$ from the hydrolysis constants ($\log k_1 = 6.48$, $\log k_2 = 11.16$, $\log k_3 = 14.16$). The results demonstrated that Pb(II) present in the forms of Pb^{2+}, $Pb(OH)^+$, $Pb(OH)_2{}^0$ and $Pb(OH)_3{}^-$ at various pH values (Fig. 7). At pH < 7.0, the main specie is Pb^{2+} and the removal of Pb^{2+} is mainly accomplished via adsorption reaction. The adsorption of Pb^{2+} can be contributed to the ion exchange between Pb^{2+} and H^+/Na^+ on the surface ion exchange sites. In the range of pH 7.0–10.0, the removal of Pb(II) maintains a high level and reaches maximum. The predominant species at pH 7.0–10.0 are $Pb(OH)^+$ and $Pb(OH)_2{}^0$ and they are easily to be adsorbed on the negatively charged diatomite surface. At pH > 10.0, the main species are $Pb(OH)_2{}^0$ and $Pb(OH)_3{}^-$, hence, the decrease of Pb(II) adsorption on diatomite can be contributed partly to the competition between OH^- and $Pb(OH)_3{}^-$. The negative $Pb(OH)_3{}^-$ is difficult to be adsorbed on the negatively charged surface of diatomite at higher pH values. The precipitation constant of $Pb(OH)_{2(s)}$ is 1.2×10^{-15}, and the precipitation curve of lead at the concentration of 15 mg/L is also shown in Fig. 6. From the precipitation curve, one can see that Pb(II) begins to form precipitation at pH ~8.7 if no Pb(II) is adsorbed on diatomite. However, ~90% Pb(II) is adsorbed on diatomite at pH ~7.0, the precipitation of $Pb(OH)_2$ can be negligible because large amounts of Pb(II) are adsorbed on diatomite. From the results, the best pH range of the system to remove Pb(II) from solution using diatomite is 7.0–10.0. The plausible interpretation of Pb(II) adsorption on diatomite at pH < 7.0 is still questionable, and further studies will be carried out at the molecular level by using spectroscopic techniques such as XPS, XAFS to attain insight into the adsorption results.

It can also be seen from Fig. 6 that the adsorption of Pb(II) on diatomite at pH < 7.0 is influenced by ionic strength obviously, whereas no drastic difference of Pb(II) adsorption is found at pH > 7.0 in the three different solution concentrations of $NaClO_4$. From the above results, one can draw a conclusion that the ionic strength dependent adsorption indicates that ion exchange or outer-sphere complexation contributes to Pb(II) adsorption on diatomite at pH < 7.0, the ionic strength independent adsorption suggests that inner-sphere complexation is the main adsorption mechanism of Pb(II) on diatomite at pH > 7.0 [21].

To illustrate the variation and relationship of pH, C_e, and q_e (mg/g, the concentration of Pb(II) on solid phase), experimental data of Pb(II) adsorption in 0.1, 0.01 and 0.001 mol/L $NaClO_4$ were plotted as 3D plots of pH, C_e, and q_e (see Fig. 8). On the pH-q_e plane, the lines are very similar to that of pH-adsorption percentage (in Fig. 6); On the pH-C_e plane, the projection on the pH-C_e plane is just the inverted image of the projection on the pH-q_e plane; On the C_e–q_e plane, the projection is a straight line containing all experimental data. It is well known that the initial concentration of Pb(II) in each experimental point is the same. The following equation can

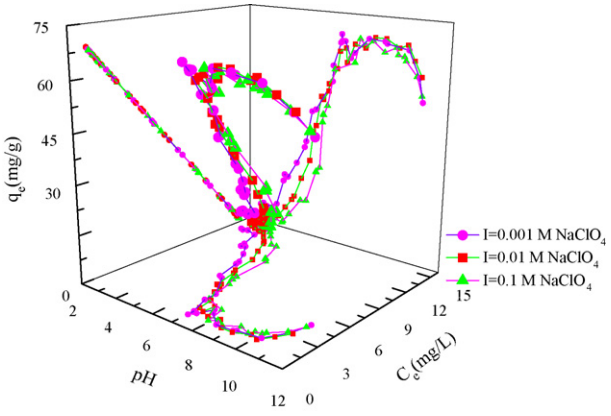

Fig. 8. 3D plots of pH, C_e and q_e of Pb(II) adsorption on diatomite, adsorbent dosage = 0.2 g/L, initial Pb(II) concentration = 15 mg/L, T = 303.15 K.

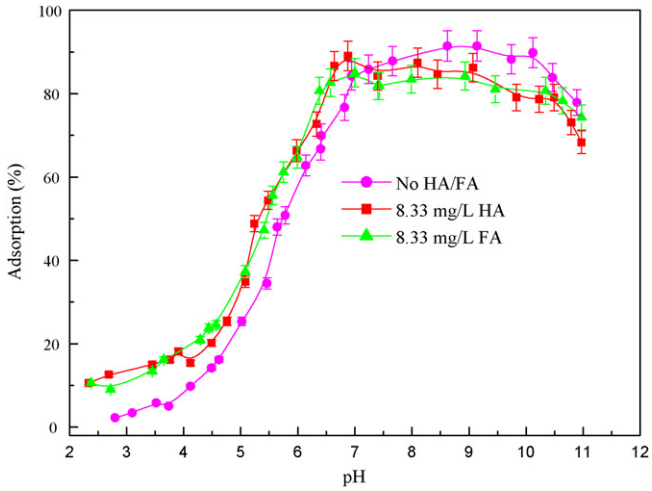

Fig. 9. Effect of HA/FA on the adsorption of Pb(II) on diatomite as a function of pH, adsorbent dosage = 0.2 g/L, initial Pb(II) concentration = 15 mg/L, I = 0.01 mol/L $NaClO_4$, T = 303.15 K.

describe the relationship of C_e–q_e:

$$VC_0 = mq_e + VC_e \quad (2)$$

Eq. (2) can be rearranged as:

$$q_e = C_0\frac{V}{m} + C_e\frac{V}{m} \quad (3)$$

where V is the volume and m is the mass of diatomite. Thereby, the experimental data of C_e–q_e lie in a straight line with a lope $(-V/m)$ and intercept (C_0V/m). The slope and intercept calculated from the C_e–q_e line are −5 and 75, which are quite in accordance with the values of V/m = 5 (L/g) and C_0V/m = 75 (mg/L × L/g) (i.e., the values calculated from V/m = 5 L/g and C_0 = 15 mg/L). The 3D plots show the relationship of pH, C_e, and q_e very clearly, i.e., all the data of C_e–q_e lie in a straight line with slope $-V/m$ and intercept C_0V/m for the same initial concentration of Pb(II) and the same diatomite content.

3.3. Effect of HA/FA

Fig. 9 illustrates the pH dependent of Pb(II) adsorption on diatomite in the absence and presence of HA/FA. As can be seen from Fig. 9, a positive effect of HA/FA on the adsorption of Pb(II) on diatomite is observed at pH < 7.0, while a negative effect of HA/FA on the adsorption of Pb(II) on diatomite is observed at pH > 7.0. HA/FA has a macromolecular structure, only a small fraction of the "adsorbed" groups is free to interact with metal ions [35]. The complexation between Pb(II) and HA/FA is more stronger than that between Pb(II) and diatomite. The free energy of the formation of HA/FA–Pb(II) complex is smaller than that of diatomite–Pb(II). Besides, at low pH values, the negative charged HA/FA can be easily adsorbed, so the strong complexation ability of surface adsorbed HA/FA with Pb(II) should result in the adsorption of Pb(II) on diatomite surface increasing at pH < 7.0. Generally, the presence of HA/FA promotes the adsorption of metal ions at low pH values while declines the adsorption at high pH values [36,37]. At pH > 7.0, the negative charged HA/FA is difficult to be adsorbed on diatomite. The HA/FA in solution forms soluble complexes of HA/FA–Pb(II), and thereby reduces Pb(II) adsorption on diatomite. Abate and Masini [38] studied Pb(II) adsorption onto vermiculite and found that the presence of HA promoted the adsorption of Pb(II) at pH 5.0 and 6.0 but suppressed the adsorption at pH 7.0 as a consequence of the formation of stable complexes in solution. Tan et al. [39] found that the presence of HA enhanced Pb(II) adsorption obviously at pH < 6.5, whereas little difference on the adsorption of Pb(II) on bare and HA

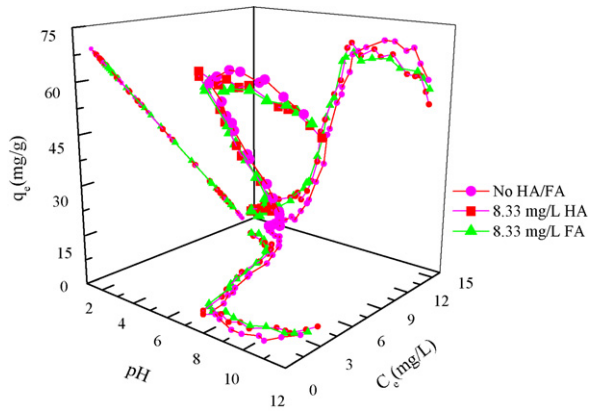

Fig. 10. 3D plots of Pb(II) adsorption on diatomite as a function of pH in the presence and absence of HA/FA, adsorbent dosage = 0.2 g/L, initial Pb(II) concentration = 15 mg/L, I = 0.01 mol/L $NaClO_4$, T = 303.15 K.

bound to rectorite was found at pH > 6.5. The results of this work are very similar to the results of the references [25,38]. It is very interesting to note that the adsorption curve of Pb(II) on diatomite in the presence of HA is quite similar to that of Pb(II) in the presence of FA. HA and FA are chemically heterogeneous compounds containing different types of functional groups at different proportions and configurations. HA and FA contain carboxyl groups (–COOH), phenolic groups (Ar–OH) and amine groups ($-NH_2$) [25], and these functional groups play a key role in affecting Pb(II) adsorption on diatomite. The samples of HA and FA were extracted from the same soil and they have similar functional groups such as carboxyl and phenolic groups. These similar functional groups may interpret the similar adsorption curve of Pb(II) on diatomite in the presence of HA/FA.

Fig. 10 illustrates the variation and relationship of pH, C_e, and q_e in Fig. 9 as 3D plots of q_e, C_e, and pH. One can clearly see that the 3D plots in Fig. 10 are quite similar to that in Fig. 8.

3.4. Effect of cations

In order to investigate the effect of cations on Pb(II) adsorption, the adsorption of Pb(II) on bare diatomite was carried out in 0.01 mol/L $NaClO_4$ and $KClO_4$ solutions, respectively, as a function of pH. As is illustrated in Fig. 11, the cations influence the adsorption of Pb(II) on diatomite drastically at pH < 8. One can see that the adsorption curve shifts to left in $KClO_4$ solution as compared

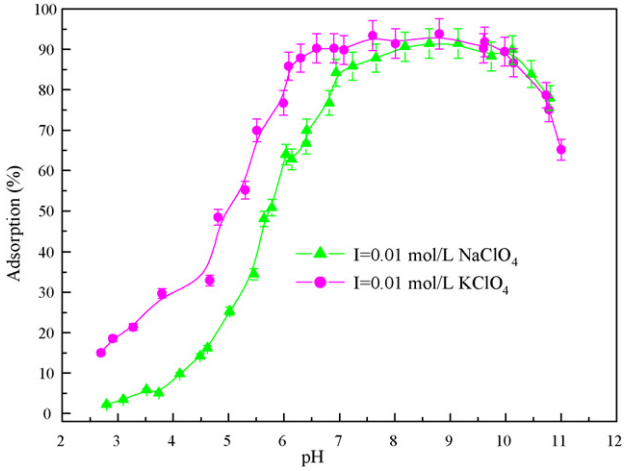

Fig. 11. Effect of cations on the adsorption of Pb(II) on diatomite as a function of pH, adsorbent dosage = 0.2 g/L, initial Pb(II) concentration = 15 mg/L, T = 303.15 K.

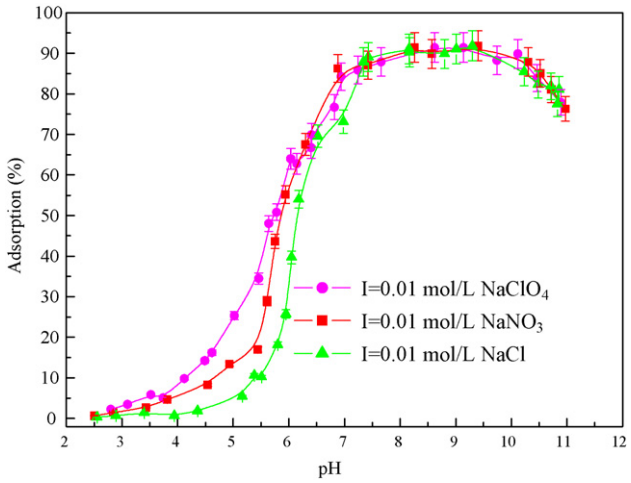

Fig. 12. Effect of anions on the adsorption of Pb(II) on diatomite as a function of pH, adsorbent dosage = 0.2 g/L, initial Pb(II) concentration = 15 mg/L, T = 303.15 K.

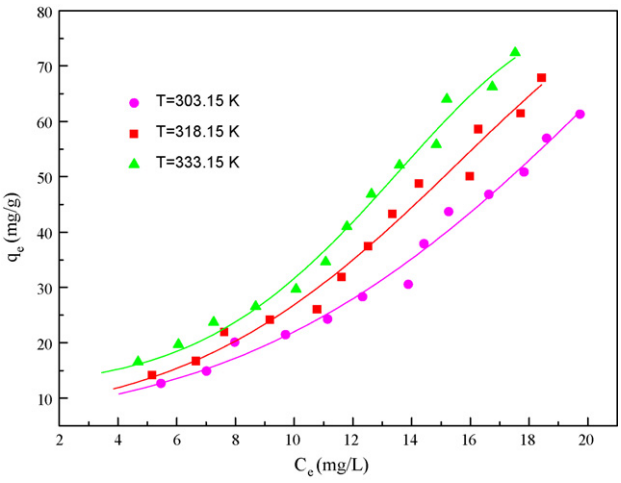

Fig. 13. Adsorption isotherms of Pb(II) to diatomite at three different temperatures, adsorbent dosage = 0.2 g/L, pH 5.20 ± 0.02, initial Pb(II) concentration = 6–32 mg/L, I = 0.01 mol/L $NaClO_4$.

to the adsorption curve in $NaClO_4$ solution, indicating that the cations can change the surface property of diatomite and hence influence the interaction of Pb(II) on diatomite surfaces. Before the addition of Pb(II), K^+/Na^+ has achieved adsorption equilibration on diatomite surface, thus the adsorption of Pb(II) on diatomite may be considered as an exchange of Pb(II) with surface adsorbed K^+/Na^+. According to Fig. 11, as supported by this competition principle, the order of removal percentage of Pb(II) to diatomite is higher for K^+ than that for Na^+, which might be ascribed to the fact that the radius of K^+ (2.32 Å) is smaller than that of Na^+ (2.76 Å) [40]. Therefore, Na^+ has higher affinity to the surface of diatomite and higher tendency for counter-ion exchange with the surface active sites of diatomite, which reduces ion interaction sites on the surface of diatomite with Pb(II). However, at pH > 8, no drastic difference of Pb(II) adsorption in $NaClO_4$ and $KClO_4$ solutions is observed, which may be attributed to the inner-sphere surface complexation at high pH values as mentioned in above section. Chen and Wang [21] investigated the effect of Na^+ and K^+ on the adsorption of Th(IV) on γ-Al_2O_3, and similar results were also found.

3.5. Effect of anions

Fig. 12 shows the adsorption curve of Pb(II) on diatomite as a function of pH in 0.01 mol/L $NaClO_4$, $NaNO_3$ and NaCl solutions, respectively. The results demonstrate that anions affect Pb(II) adsorption drastically at pH < 8, the adsorption percentage of Pb(II) on diatomite is the lowest in NaCl solution and the highest in $NaClO_4$ solution. This phenomenon may be contributed to the facts that: (I) Cl^- and NO_3^- can form soluble complexes with Pb(II) ion in solution (e.g. $PbCl_x^{(2-x)-}$, $Pb(NO_3)_x^{(2-x)-}$), while ClO_4^- does not form soluble complexes with Pb(II) in solution. Pb(II) has the highest affinity to Cl^- but the lowest affinity to ClO_4^-; (II) Idiocratic adsorption of Cl^- to diatomite surface is a little easier than NO_3^- and ClO_4^-, and Cl^- adsorption on the surface of diatomite changes the surface properties of diatomite and decreases the availability of binding sites for Pb(II); (III) The inorganic acid radicals radium sequence is $Cl^- < NO_3^- < ClO_4^-$, the smaller radium inorganic acid radicals can take up more ionic exchange sites and lead to the decline of Pb(II) adsorption on diatomite [21].

3.6. Effect of temperature and thermodynamic data

The adsorption isotherms of Pb(II) on diatomite at T = 303.15, 318.15 and 333.15 K are shown in Fig. 13. The adsorption isotherm is the highest at T = 333.15 K and is the lowest at T = 303.15 K, illustrating that the adsorption of Pb(II) on diatomite is promoted at higher temperature. One possible interpretation of this phenomenon is that the Pb(II) ions are well hydrated, to be adsorbed on diatomite, they have to lose the hydration shell which needs energy, so the removal of water molecules from Pb(II) ions is an endothermic process in essence [42]. Xu et al. [41] studied the temperature dependent adsorption of Ni^{2+} on Na-montmorillonite. Chen and Wang [42] studied the temperature dependent adsorption of Ni^{2+} to oxidized multiwall carbon nanotubes, and similar results were reported.

The Freundlich isotherm model is applied to describe the adsorption characteristics of Pb(II) on diatomite. The Freundlich isotherm model is responsible for several kinds of adsorption sites on the diatomite surface and illustrates properly the adsorption data at low and intermediate concentrations on heterogeneous surfaces. The model has the following form [22,43]:

$$q_e = k_F C_e^{\,n} \tag{4}$$

Eq. (4) can also be expressed in the linear form:

$$\log q_e = \log k_F + n \log C_e \tag{5}$$

where k_F ($mg^{1-n}\,g^{-1}\,L^n$) represents the adsorption capacity and n represents the degree of dependence of adsorption at equilibrium concentration.

The Freundlich adsorption isotherm of Pb(II) to diatomite at T = 303.15, 318.15 and 333.15 K is shown in Fig. 14. The experimental data are well fitted by the Freundlich model. The relative parameters calculated from the Freundlich model are listed in Table 2. A comparison of the Freundlich adsorption capacity of diatomite studied in this work with that of other common adsorbents such as carbon nanotubes [7] and activated carbon [3] documented in the literatures shows that the adsorption capacity of diatomite for Pb(II) is much higher than that of carbon nanotubes and activated carbon. Thus, considering the lower cost of this natural adsorbent,

Table 2
Constants of Freundlich isotherm adsorption of Pb(II) on diatomite.

T (K)	Freundlich model		
	k_F ($mg^{1-n}\,g^{-1}\,L^n$)	n	R
303.15	8.07	1.403	0.972
318.15	14.86	1.383	0.978
333.15	47.64	1.308	0.977

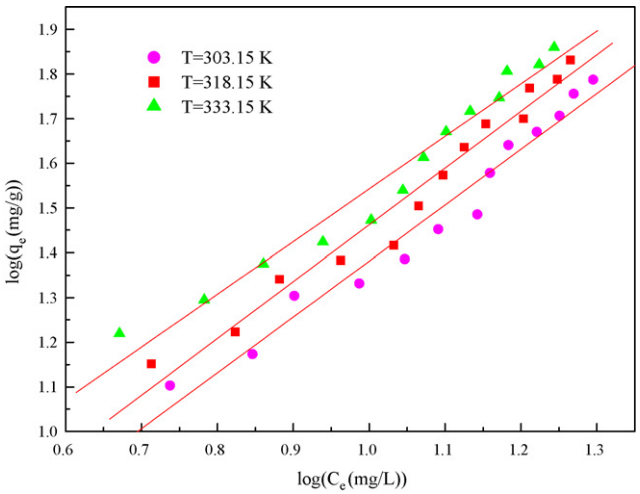

Fig. 14. Freundlich fitting isotherms for Pb(II) adsorption on diatomite at three different temperatures, adsorbent dosage = 0.2 g/L, pH 5.20 ± 0.02, initial Pb(II) concentration = 6–32 mg/L, I = 0.01 mol/L $NaClO_4$.

diatomite can be used as an alternative material to eliminate Pb(II) from wastewater.

The thermodynamic parameters (ΔH°, ΔS°, and ΔG°) for Pb(II) adsorption on diatomite can be calculated from the temperature dependent adsorption. The values of enthalpy (ΔH°) and entropy (ΔS°) can be calculated from the slope and y-intercept of the plot of $\ln K_d$ vs. $1/T$ (Fig. 15) via applying the following equations:

$$K_d = \frac{C_0 - C_e}{C_e}\frac{V}{m} \quad (6)$$

$$\ln K_d = \frac{\Delta S^\circ}{R} - \frac{\Delta H^\circ}{RT} \quad (7)$$

where C_0 is the initial concentration (mg/L), C_e is the equilibration concentration after centrifugation (mg/L), V is the volume (mL) and m is the mass of diatomite (g), R (8.314 J mol^{-1} K^{-1}) is the ideal gas constant, and T (K) is the temperature in Kelvin.

Free energy changes (ΔG°) of specific adsorption are calculated from:

$$\Delta G^\circ = \Delta H^\circ - T\Delta S^\circ \quad (8)$$

Relevant data attained from Eqs. (7) and (8) are given in Table 3. The evaluation of thermodynamic parameters provides an insight

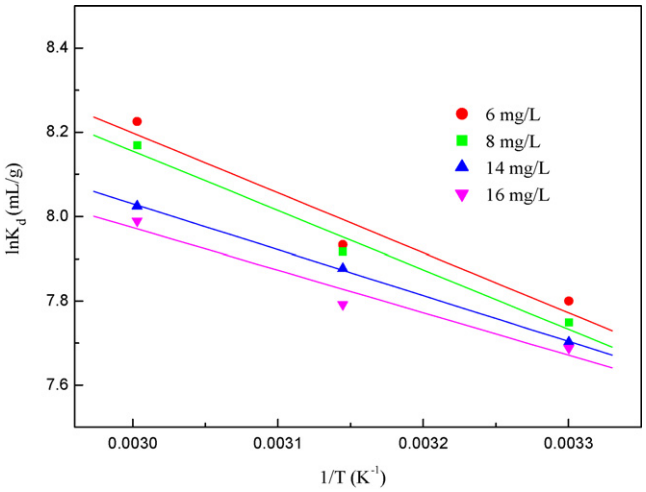

Fig. 15. The linear plot of $\ln K_d$ vs. $1/T$ for Pb(II) adsorption on diatomite, adsorbent dosage = 0.2 g/L, pH 5.20 ± 0.02, I = 0.01 mol/L $NaClO_4$.

Table 3
Values of thermodynamic parameters for the adsorption of Pb(II) on diatomite.

C_0 (mg L^{-1})	ΔH° (kJ mol^{-1})	ΔS° (J mol^{-1} K^{-1})	ΔG° (kJ mol^{-1})		
			303.15 K	318.15 K	333.15 K
6	11.66	103.6	−19.65	−20.97	−22.77
8	11.70	102.9	−19.52	−20.93	−22.62
14	9.03	93.85	−19.40	−20.60	−22.22
16	8.38	91.17	−19.37	−20.60	−22.12

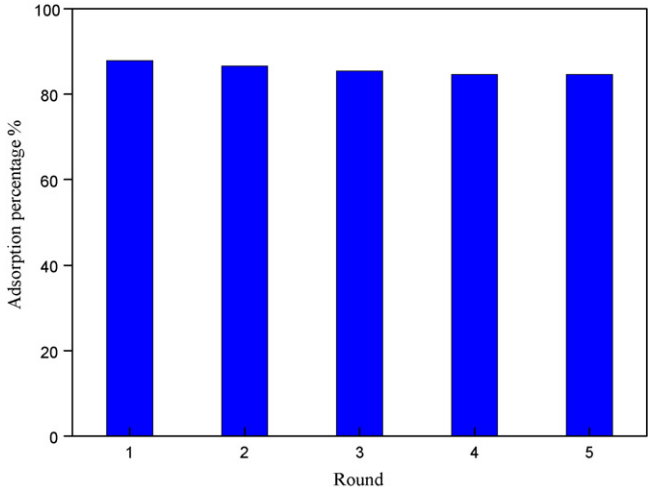

Fig. 16. Recycling of diatomite in the removal of Pb(II).

into the mechanism of Pb(II) adsorption to diatomite. As is expected for a spontaneous process under the experimental conditions, it is clear that the free energy of Pb(II) adsorption on diatomite is more negative at higher temperature, which demonstrates that the spontaneity of the adsorption process increases with the rise in temperature. A positive value of the standard enthalpy change (ΔH°) indicates that the adsorption process is endothermic. The low value of ΔH° also suggests that the endothermic process of Pb(II) adsorption on diatomite is weak. This conclusion is supported by the weakly increasing adsorption with the increase in temperature. As the free energy changes are negative and accompanied by positive entropy changes, the adsorption reactions are spontaneous with a high affinity.

3.7. Regeneration

The repeated availability of diatomite for Pb(II) adsorption through many cycles of adsorption/desorption is quite crucial for the application of diatomite in the removal of Pb(II) from wastewater in real work. Herein, the recycling of diatomite in the removal of Pb(II) was investigated. We found that the recycling was valid for at least five times as shown in Fig. 16 to give a satisfied removal percentage even in the fifth round. This result suggests that the diatomite can be employed repeatedly in Pb(II) adsorption.

4. Conclusions

Based on the results attained in this work, the following conclusions can be obtained:

(1) Adsorption of Pb(II) on diatomite is strongly dependent on pH in the range of 2–12. The adsorption is dependent on ionic strength at pH < 7.0, and independent of ionic strength at pH > 7.0.
(2) Outer-sphere surface complexation or ion exchange may be the main adsorption mechanism of Pb(II) on diatomite at pH < 7.0,

whereas the adsorption of Pb(II) at pH > 7.0 is mainly dominated by inner-sphere surface complexation.

(3) The presence of HA/FA enhances Pb(II) adsorption on diatomite at pH < 8.0, but suppresses Pb(II) adsorption on diatomite at pH > 8.0.
(4) The cations or anions influence the adsorption of Pb(II) on diatomite obviously at pH < 8.0, and no influence is found at pH > 8.0.
(5) The adsorption isotherms of Pb(II) on diatomite can be described well by the Freundlich model.
(6) The thermodynamic parameters calculated from the temperature dependent adsorption isotherms indicate that the adsorption process is spontaneous and endothermic.
(7) The high adsorption capacity of diatomite makes it a suitable material in the removal of heavy metals from large volume solutions for the practical application in wastewater treatment.

Acknowledgements

Financial support from the National Natural Science Foundation of China (20677058; 20501019) and 973 project (2007CB936602) is acknowledged. Professor Han-Qing Yu from Laboratory of Environmental Science and Engineering, the University of Science & Technology of China, is greatly appreciated for the measurement of Zeta potentials.

References

[1] J.O. Nriagu, J.M. Pacyna, Quantitative assessment of worldwide contamination of air, water and soils by trace metals, Nature 333 (1988) 134–139.
[2] J.F. Liu, Z.S. Zhao, G.B. Jiang, Coating Fe_3O_4 magnetic nanoparticles with humic acid for high efficient removal of heavy metals in water, Environ. Sci. Technol. 42 (2008) 6949–6954.
[3] M. Sekar, V. Sakthi, S. Rengaraj, Kinetics and equilibrium adsorption study of lead(II) on activated carbon prepared from coconut shell, J. Colloid Interface Sci. 279 (2004) 307–313.
[4] A. Demirbas, E. Pehlivan, F. Gode, T. Altun, G. Arslan, Adsorption of Cu(II), Zn(II), Ni(II), Pb(II), and Cd(II) from aqueous solution on Amberlite IR-120 synthetic resin, J. Colloid Interface Sci. 282 (2005) 20–25.
[5] X. Feng, G.E. Fryxell, L.Q. Wang, A.Y. Kim, J. Liu, K.M. Kemner, Functionalized monolayers on ordered mesoporous supports, Science 276 (1997) 923–926.
[6] Y.H. Li, Z.C. Di, J. Ding, D.H. Wu, Z.K. Luan, Y.Q. Zhu, Adsorption thermodynamic, kinetic and desorption studies of Pb^{2+} on carbon nanotubes, Water Res. 39 (2005) 605–609.
[7] H.J. Wang, A.L. Zhou, F. Peng, H. Yu, L.F. Chen, Adsorption characteristic of acidified carbon nanotubes for heavy metal Pb(II) in aqueous solution, Mater. Sci. Eng. A 466 (2007) 201–206.
[8] S.B. Wang, T. Terdkiatburana, M.O. Tadé, Adsorption of Cu(II), Pb(II) and humic acid on natural zeolite tuff in single and binary systems, Sep. Purif. Technol. 62 (2008) 64–70.
[9] U. Wingenfelder, C. Hansen, G. Furrer, R. Schulin, Removal of heavy metals from mine waters by natural zeolites, Environ. Sci. Technol. 39 (2005) 4606–4613.
[10] A. Sari, M. Tuzen, D. Citak, M. Soylak, Equilibrium, kinetic and thermodynamic studies of adsorption of Pb(II) from aqueous solution onto Turkish kaolinite clay, J. Hazard. Mater. 149 (2007) 283–291.
[11] A. Sari, M. Tuzen, M. Soylak, Adsorption of Pb(II) and Cr(III) from aqueous solution on Celtek clay, J. Hazard. Mater. 144 (2007) 41–46.
[12] S.Q. Zhang, W.G. Hou, Adsorption behavior of Pb(II) on montmorillonite, Colloids Surf. A: Physicochem. Eng. Aspects 320 (2008) 92–97.
[13] A.E. Osmanlioglu, Natural diatomite process for removal of radioactivity from liquid waste, Appl. Radiat. Isot. 65 (2007) 17–20.
[14] M.A.M. Khraisheh, Y.S. Al-degs, W.A.M. Mcminn, Remediation of wastewater containing heavy metals using raw and modified diatomite, Chem. Eng. J. 99 (2004) 177–184.
[15] Z. Reddad, C. Gerente, Y. Andres, P. Le Cloirec, Adsorption of several metal ions onto a low-cost biosorbent: kinetic and equilibrium studies, Environ. Sci. Technol. 36 (2002) 2067–2073.
[16] T.N.D.C. Dantas, A.A.D. Neto, M.C.P.D. Moura, Removal of chromium from aqueous solutions by diatomite treated with micro emulsion, Water Res. 35 (2001) 2219–2224.
[17] M. Gürü, D. Venedik, A. Murathan, Removal of trivalent chromium from water using low-cost natural diatomite, J. Hazard. Mater. 160 (2008) 318–323.
[18] Y. Al-Degs, M.A.M. Khraisheh, M.F. Tutunji, Sorption of lead ions on diatomite and manganese oxides modified diatomite, Water Res. 15 (2001) 3724–3728.
[19] M.A.M. Khraisheh, M.A. Al-Ghouti, S.J. Allen, M.N. Ahmad, Effect of OH and silanol groups in the removal of dyes from aqueous solution using diatomite, Water Res. 39 (2005) 922–932.
[20] Y.X. Yang, J.B. Zhang, W.M. Yang, J.D. Wu, R.S. Chen, Adsorption properties for urokinase on local diatomite surface, Appl. Surf. Sci. 206 (2003) 20–28.
[21] C.L. Chen, X.K. Wang, Influence of pH, soil humic/fulvic acid, ionic strength and foreign ions on adsorption of thorium(IV) onto γ-Al_2O_3, Appl. Geochem. 22 (2007) 436–445.
[22] X.L. Tan, X.K. Wang, C.L. Chen, A.H. Sun, Effect of soil humic and fulvic acids, pH and ionic strength on Th(IV) sorption to TiO_2 nanoparticles, Appl. Radiat. Isot. 65 (2007) 375–381.
[23] D. Xu, X.K. Wang, C.L. Chen, X. Zhou, X.L. Tan, Influence of soil humic acid and fulvic acid on adsorption of thorium(IV) on MX-80 betonite, Radiochim. Acta 94 (2006) 429–434.
[24] D. Xu, D.D. Shao, C.L. Chen, A.P. Ren, X.K. Wang, Effect of pH and fulvic acid on adsorption and complexation of cobalt onto bare and FA bound MX-80 bentonite, Radiochim. Acta 94 (2006) 97–102.
[25] X.L. Tan, X.K. Wang, H. Geckeis, T.H. Rabung, Sorption of Eu(III) on humic acid or fulvic acid bound to alumina studied by SEM-EDS, XPS, TRLFS and batch techniques, Environ. Sci. Technol. 42 (2008) 6532–6537.
[26] Z.Y. Tao, J. Zhang, J. Zhai, Characterization and differentiation of humic acids and fulvic acids in soils from various regions of China by nuclear magnetic resonance spectroscopy, Anal. Chim. Acta 395 (1999) 199–203.
[27] J. Zhang, J.J. Zhai, F.Z. Zhao, Z.Y. Tao, Study of soil humic substances by cross-polarization magic angle spinning ^{13}C nuclear magnetic resonance and pyrolysis-capillary gas chromatography, Anal. Chim. Acta 378 (1999) 177–182.
[28] Y.P. Chin, G. Alken, E. O'Loughlin, Molecular weight, polydispersity, and spectroscopic properties of aquatic humic substances, Environ. Sci. Technol. 28 (1994) 1853–1858.
[29] S. Bratskaya, A. Golikov, T. Lutsenko, O. Nesterova, V. Dudarchik, Charge characteristics of humic and fulvic acids: comparative analysis by colloid titration and potentiometric titration with continuous pK-distribution function model, Chemosphere 73 (2008) 557–563.
[30] R. Köseoglu, F. Köksal, E. Ciftci, M. Akkurt, Identification of paramagnetic radicals in γ-irradiated natural diatomite minerals by electron paramagnetic resonance, J. Mol. Struct. 733 (2005) 151–154.
[31] J. Huang, Y. Liu, Q. Jin, X. Wang, J. Yang, Adsorption studies of a water soluble dye, reactive red MF-3B, using sonication-surfactant-modified attapulgite clay, J. Hazard. Mater. 143 (2007) 541–548.
[32] B. Lee, D. Lu, J.N. Kondo, K. Domen, Three-dimensionally ordered mesoporous niobium oxide, J. Am. Chem. Soc. 124 (2002) 11256–11257.
[33] B.J. Gao, P.F. Jiang, F.Q. An, S.Y. Zhao, Z. Ge, Studies on the surface modification of diatomite with polyethyleneimine and trapping effect of the modified diatomite for phenol, Appl. Clay Sci. 250 (2005) 273–279.
[34] C.H. Weng, Modeling Pb(II) adsorption onto sandy loam soil, J. Colloid Interface Sci. 272 (2004) 262–270.
[35] T.J. Strathmann, S.C.B. Myneni, Effect of soil fulvic acid on nickel(II) sorption and bonding at the aqueous-boehmite(γ-AlOOH) interface, Environ. Sci. Technol. 39 (2005) 4027–4034.
[36] G. Montavon, S. Markai, Y. Andres, B. Grambow, Complexation studies of Eu(III) with alumina-bound polymaleic acid: effect of organic polymer loading and metal ion concentration, Environ. Sci. Technol. 36 (2002) 3303–3309.
[37] Y. Takahashi, Y. Minai, S. Ambe, Y. Makide, F. Ambe, Comparison of adsorption behavior of multiple inorganic ions on kaolinite and silica in the presence of humic acid using the multitracer technique, Geochim. Cosmochim. Acta 63 (1999) 815–836.
[38] G. Abate, J.C. Masini, Influence of pH, ionic strength and humic acid on adsorption of Cd(II) and Pb(II) onto vermiculite, Colloids Surf. A: Physicochem. Eng. Aspects 262 (2005) 33–39.
[39] X.L. Tan, P.P. Chang, Q.H. Fan, X. Zhou, S.M. Yu, W.S. Wu, X.K. Wang, Sorption of Pb(II) on Na-rectorite: effects of pH, ionic strength, temperature, soil humic acid and fulvic acid, Colloids Surf. A: Physicochem. Eng. Aspects 328 (2008) 8–14.
[40] F. Esmadi, J. Simm, Adsorption of cobalt(II) by amorphous ferric hydroxide, Colloids Surf. A: Physicochem. Eng. Aspects 104 (1995) 265–270.
[41] D. Xu, X. Zhou, X.K. Wang, Adsorption and desorption of Ni^{2+} on Na-montmorillonite: effect of pH, ionic strength, fulvic acid, humic acid and addition sequences, Appl. Clay Sci. 39 (2008) 133–141.
[42] C.L. Chen, X.K. Wang, Adsorption of Ni(II) from aqueous solution using oxidized multiwall carbon nanotubes, Ind. Eng. Chem. Res. 45 (2006) 9144–9149.
[43] X.L. Tan, X.K. Wang, M. Fang, C.L. Chen, Sorption and desorption of Th(IV) on nanoparticles of anatase studied by batch and spectroscopy methods, Colloids Surf. A: Physicochem. Eng. Aspects 296 (2007) 109–116.